Cell Reports
Article

Polyester Modification of the Mammalian TRPM8 Channel Protein: Implications for Structure and Function

Chike Cao,[1,7] Yevgen Yudin,[1,7] Yann Bikard,[1] Wei Chen,[2] Tong Liu,[2] Hong Li,[2] Dieter Jendrossek,[3] Alejandro Cohen,[4] Evgeny Pavlov,[5] Tibor Rohacs,[1] and Eleonora Zakharian[1,6,*]

[1]Department of Pharmacology and Physiology, New Jersey Medical School, UMDNJ, 185 South Orange Avenue, MSB H626, Newark, NJ 07103, USA

[2]Center for Advanced Proteomics Research, New Jersey Medical School Cancer Center, UMDNJ, Building F1105, 205 South Orange Avenue, Newark, NJ 07103, USA

[3]Universität Stuttgart Zentrum für Bioverfahrenstechnik, Institut für Mikrobiologie, Allmandring 31, 70569 Stuttgart, Germany

[4]Proteomics Core Facility, Clinical Research Centre, Dalhousie University, Room C-304, 5849 University Avenue, P.O. Box 15000, Halifax NS B3H 4R2, Canada

[5]Department of Physiology and Biophysics Faculty of Medicine, Dalhousie University, Sir Charles Tupper Medical Building, Room 5G, 5850 College Street, Halifax NS B3H 4R2, Canada

[6]Department of Cancer Biology and Pharmacology, University of Illinois College of Medicine, 1 Illini Drive, Peoria, IL 61605, USA

[7]These authors contributed equally to this work

*Correspondence: zakharel@uic.edu

http://dx.doi.org/10.1016/j.celrep.2013.06.022

SUMMARY

The TRPM8 ion channel is expressed in sensory neurons and is responsible for sensing environmental cues, such as cold temperatures and chemical compounds, including menthol and icilin. The channel functional activity is regulated by various physical and chemical factors and is likely to be preconditioned by its molecular composition. Our studies indicate that the TRPM8 channel forms a structural-functional complex with the polyester poly-(R)-3-hydroxybutyrate (PHB). We identified by mass spectrometry a number of PHB-modified peptides in the N terminus of the TRPM8 protein and in its extracellular S3-S4 linker. Removal of PHB by enzymatic hydrolysis and site-directed mutagenesis of both the serine residues that serve as covalent anchors for PHB and adjacent hydrophobic residues that interact with the methyl groups of the polymer resulted in significant inhibition of TRPM8 channel activity. We conclude that the TRPM8 channel undergoes posttranslational modification by PHB and that this modification is required for its normal function.

INTRODUCTION

Posttranslational modifications of proteins, such as glycosylation, nitrosylation, or phosphorylation, are widespread phenomena in cellular physiology. Here, we report a posttranslational modification of the transient receptor potential protein, TRPM8, by a polyester comprised of repeated units of R-3-hydroxybutyrate, which forms a polymeric chain, poly-(R)-3-hydroxybutyrate (PHB). We term this modification PHBylation by analogy with the established protein modifications.

TRPM8 is a member of the transient receptor potential (TRP) channel family of the melastatin subgroup. TRPM8 is a major sensor for a wide range of cold temperatures in the peripheral nervous system (Bautista et al., 2007; Colburn et al., 2007; Dhaka et al., 2007). In recombinant expression systems, the channel is activated by low temperatures in the range of 10°C –28°C and by a number of chemical compounds, such as menthol, icilin, eucalyptol, geraniol, and linalool (Behrendt et al., 2004; McKemy et al., 2002; Peier et al., 2002).

PHB may form supramolecular complexes with proteins via covalent bonds and multiple hydrophobic interaction sites (Reusch, 1989, 1999; Seebach et al., 1994). The physical properties and large size of the polyester may have substantial structural and functional impacts on the protein. The high-energy C-terminal coenzyme A (CoA)-ester group derived from PHB metabolic precursors presumably acts as a cofactor for the enzymatic reaction in which a covalent bond to the protein is formed (Zhang et al., 2011).

Originally, protein/PHB complexes were discovered in bacteria, where they are postulated to play roles in protein folding, protein sorting, or retention of inorganic polyphosphate (polyP) (Negoda et al., 2010; Xian et al., 2007). In a recent study (Zakharian et al., 2009), we found that the TRPM8 channel forms a functionally important ionic complex with polyP under native conditions. Moreover, western blot analysis with PHB antibodies indicated that the TRPM8 protein might also contain PHB. However, the role and specific sites of the molecular interaction between PHB and TRPM8 remained unclear.

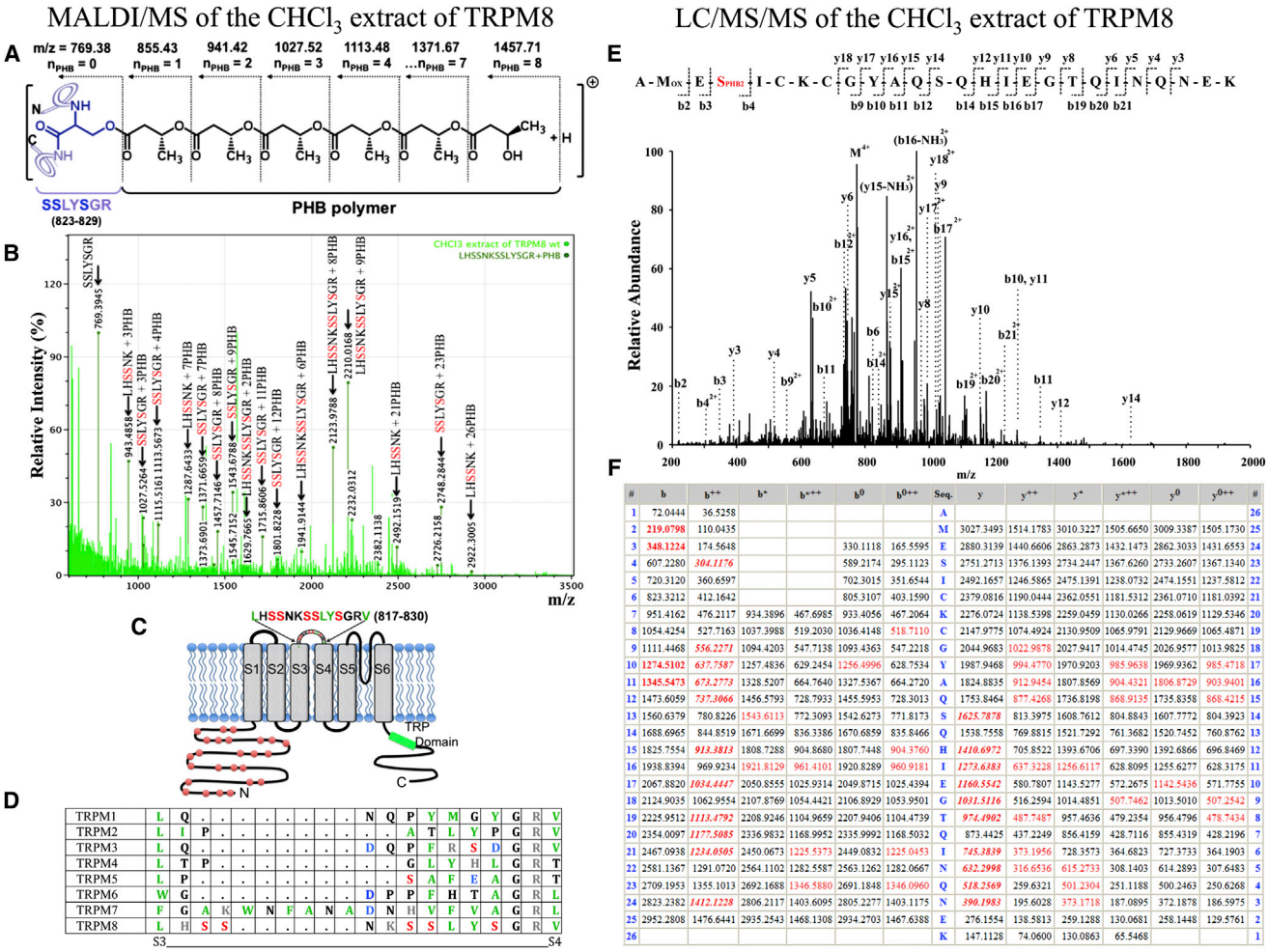

Figure 1. Mass Spectrometric Analysis of the Chloroform-Extracted Peptide LHSSNKSSLYSGR 817–829 of the TRPM8 Protein Derived from MALDI/MS Experiments

(A) Molecular composition of PHBylated serine residue on the SSLYSGR (823–829) peptide with a number of PHB units attached via an ester bond; numbers indicate the PHB modification with a shift in the monoisotopic masses.

(B) Intensity peaks of the LHSSNKSSLYSGR (817–829) peptide with indicated PHB modifications detected in mass spectrum of the chloroform-extracted peptides derived from MALDI/MS. Masses were analyzed with the ExPASy FindMod Tool (SWISS-PROTeomics Bioinformatics Resources) run against the TRPM8 sequence with possible PHB modifications up to 30 units, with zero or one missed cleavage cites for trypsin-digested protein (error window ± 50 ppm). The variability of different lengths of PHB might be due to the breakage of labile ester bonds under the MS laser beam (Xian et al., 2007).

(C) Cartoon of the putative PHB-modification sites on the TRPM8 protein with a sequence indication for the extracellular PHBylated peptides. The red spheres indicate putative PHBylated peptides on the N terminus of TRPM8 derived from MALDI-MS experiments.

(D) The amino acid sequence of the S3-S4 linker of TRPM family ion channels is not conserved.

(E) MS/MS spectrum of the quadruply charged ion (m/z 775.354) corresponding to the peptide ^{63}AMESICKCGYAQSQHIEGTQINQNEK^{88} showing the methionine oxidation and two units of PHB modification on serine residues. The observed *y*- and *b*-ion series confirmed the peptide sequence. The *b4, b9, b10, b11, b12, b14, b15, b16, b17, b19, b20*, and b21 ions confirmed PHB localization on the serine residue.

(F) A table showing the identified peptide fragment ions from the spectrum (red) versus theoretical fragment ions not found in the spectrum (black). The bold italic red ions are the relatively abundant y- or b-ions that contributed to the scoring of the peptide and posttranslational modifications identification. Additional matched ions, including bold red ions, were not used for the calculation of the identification score.

See also Figure S1 and S4.

The PHB molecule is comprised of hydrophobic methyl groups alternating with hydrophilic ester groups and has a CoA-ester binding group at its C-terminal end (Figures 1A and S1). The metabolic pathway for PHB synthesis in eukaryotes is not well understood, but might be similar to that for cholesterol. Both PHB and cholesterol share a common intermediate, acetoacetyl-CoA, and their synthesis is regulated by changes in intracellular concentrations of acetyl-CoA (Norris et al., 2009). Acetoacetate and 3-hydroxybutyrate are well-known physiological compounds in higher eukaryotes.

The molecular structure of the PHB polymer creates a highly flexible carbon backbone with a lipophilic outer surface

(Cornibert and Marchessault, 1972). Upon association with proteins, the high hydrophobicity of the polyester may substantially alter their physical properties and thus affect their function. This may also be the case for the TRPM8 protein, in which association of the cold receptor with PHB may define its thermodynamic properties.

To reveal the physiological role(s) of the association of the PHB polymer with TRPM8, we performed mass-spectrometric analysis of the TRPM8 protein and identified a substantial number of putative PHB-modified peptides throughout the channel. The majority of these peptides reside on the N terminus of TRPM8; however, one PHB-modification site was found on the extracellular side of the channel. Here, we focus on this extracellular PHBylated peptide of TRPM8. We mutated several serines on this peptide, which is located in the putative loop between the third and fourth transmembrane domains (S3-S4 linker). We find that the mutants with deleted PHB-modification sites show no difference in their expression or localization, but their channel function is severely affected. Our data suggest that PHB is a structural component of the TRPM8 protein and that PHB is required for channel activity.

RESULTS

Mass Spectrometry Analysis of the TRPM8 Protein

Western blot analysis of TRPM8 immunoblotted with PHB antibodies suggested that TRPM8 is conjugated with PHB (Zakharian et al., 2009). Here, we have performed a detailed analysis of the immunoprecipitated TRPM8 protein by mass spectrometry, including matrix-assisted laser desorption/ionization (MALDI) mass spectrometry (MS), to identify peptides with potential PHB modifications. We found that PHB was associated with specific serine residues on these peptides, possibly via formation of ester bonds (Figure S2).

To distinguish true from false candidates among the large number of PHBylated peptides derived from MALDI/MS, we further separated the peptides into two distinct groups—hydrophilic and hydrophobic. This was accomplished by extraction of the aqueous solution of trypsin-digested TRPM8 peptides with chloroform. Association with PHB may render amphiphilic or even hydrophilic peptides soluble in chloroform (Castuma et al., 1995; Pavlov et al., 2005; Seebach and Fritz, 1999). The 1:1 aqueous/chloroform mixture was incubated overnight at room temperature with slow rotation to allow complete separation of the fractions and extraction of the hydrophobic from hydrophilic substances. The hydrophobic fraction was then carefully separated, avoiding contamination from the interphase region, and the peptides were then examined by MALDI/MS. We found that the majority of the peptides that had been identified as modified before partitioning were extracted into the chloroform layer (Figure S3). The intensity peaks obtained by MALDI/MS for the peptides are presented in the lower panel of Figure S3.

The majority of putative PHB-modification sites were found throughout the N terminus of TRPM8, and one modification was found on the extracellular side of the channel (Figures 1B and S4). Figure 1B shows the distribution of the peaks obtained for two consecutive PHBylated peptides, LHSSNK (817–822) and SSLYSGR (823–829), which are located in the S3-S4 linker. PHB modification was observed both on each separate peptide and on the entire S3-S4 linker (with one missed tryptic cleavage site). The PHB modification, including mass values that correspond to the number of PHB units attached via ester bonds to serine on SSLYSGR (823–829), is illustrated in Figure 1A, and a cartoon of the putative PHB-binding sites on the TRPM8 protein is shown in Figure 1C. The amino acid sequence in the S3-S4 linker is not conserved among the TRPM family members (Figure 1D). The representative expanded MALDI/MS spectrum from the experiments conducted on the chloroform extracts of TRPM8 is presented in Figures S4A–S4H.

To confirm the potential modifications indicated by MALDI/MS analysis (error within a range of ±50 ppm), we next performed liquid chromatography-tandem mass spectrometry (LC-MS/MS) experiments with the chloroform-extracted peptides on the Orbitrap (precursor error within a range of ±10 ppm). This process produced low-intensity peaks, due to the rupture of PHB ester bonds under the intense MS laser beam (Figure S5) and, thus, low confidence scores for the modified peptides. Nevertheless, some of the target peptides previously observed with MALDI/MS were also detected using LC-MS/MS. In particular, the peptide located on the N terminus of TRPM8 was detected with a mass shift of 172.07, which was compatible with the mass predicted for two PHB units. A representative LC-MS/MS spectrum of the PHBylated peptide with two PHB units attached to Ser66 is shown in Figure 1E. The masses of quadruply charged ions involved in this modification are presented in Figure 1F.

Next, we estimated the number of PHB units attached to each of the TRPM8 peptides. After MALDI/MS or LC-MS/MS, the PHB polymers on targeted peptides varied in length from 1 to 26 units (Figures 1 and S2–S5). We suggest that this wide range of PHB lengths is an artifact caused by breakage of the labile ester bonds of PHB under the MS beam. Rapid disintegration of the PHB polyester during MS experiments has previously been shown for the PHB-conjugated outer membrane protein A (OmpA) (Xian et al., 2007). It is possible that the original length of the polyester would be the longest polymer length observed in these experiments. However, it is difficult to determine whether the maximum length of the PHB chain associated with the TRPM8 peptides is 26 units or whether PHB is attached to more than one serine per peptide.

Mutants of PHB-Modified Serines in the S3-S4 Linker Alter TRPM8 Channel Function

MS analysis indicated a large number of TRPM8 peptides that are putatively covalently modified by PHB. The majority of these peptides are located on the intracellular N terminus. However, one PHB-modification site was identified on the extracellular side of TRPM8. Here, we focus on the physiological role of this extracellular PHB modification of TRPM8 channel (Figure 1).

After trypsin digestion, two tandem PHB-modified peptides, LHSSNK and SSLYSGR (amino acid position 817–829), were detected with the polymer attached to one or more serines per peptide (Figures 1 and S4). We performed site-directed mutagenesis to create PHB binding-site mutants for these peptides to determine what effect this alteration would have on TRPM8 channel activity. An amino acid lacking a hydroxyl group was

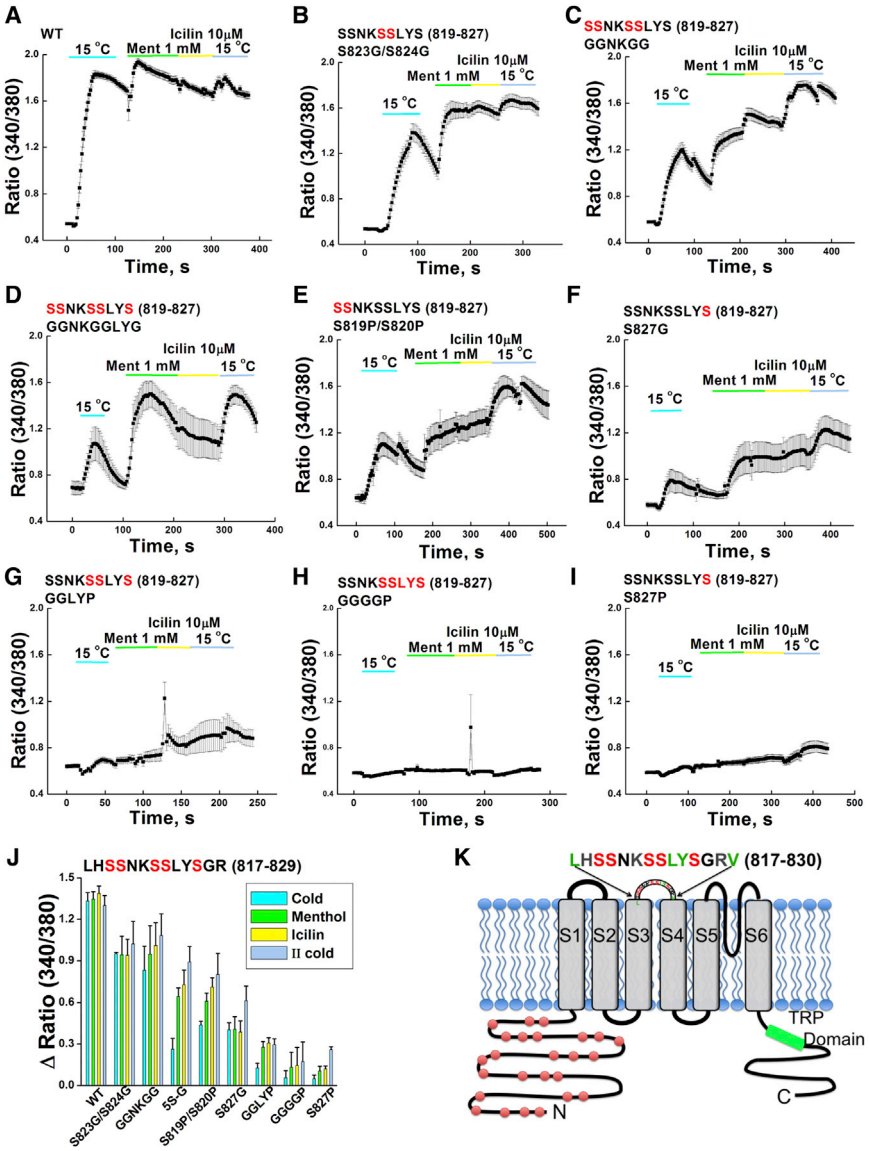

Figure 2. Screening of the Serine Mutants within the Peptide LHSSNKSSLYSGR 817–829 for TRPM8 Activity in Intracellular Ca^{2+} Measurements

Fluorescence measurements of intracellular Ca^{2+} concentration were performed on HEK293 cells transiently transfected with the wild-type or mutants TRPM8 (0.7 μg) and GFP (0.2 μg) constructs. (A–I) Representatives from single coverslips, the total number of measurements (n), and total number of cells for each variety are indicated in parentheses. (A) TRPM8 wild-type (n = 5; n_{cells} = 71); (B) double serine mutant S823G/S824G (n = 8; n_{cells} = 99); (C) quadruple serine mutant S819G/S820G/S823G/S824G or GGNKGG (n = 4; n_{cells} = 76); (D) quintuple serine mutant 5S-G: S819G/S820G/S823G/S824G/S827G or GGNKGGLYG (n = 8; n_{cells} = 61); (E) double serine mutant S819P/S820P (n = 4; n_{cells} = 53); (F) single serine mutant S827G (n = 7; n_{cells} = 171); (G) triple serine mutant S823G/S824G/S827P or GGLYP (n = 5; n_{cells} = 67); (H) quintuple serine mutant S823G/S824G/L825G/Y826G/S827P or GGGGP (n = 7; n_{cells} = 88); (I) single serine mutant S827P (n = 6; n_{cells} = 83).

(J) The summary of cold, menthol, icilin, and second cold applications (error bars stand for ± SEM). Alternatively, these measurements were carried with a single application of icilin, which resulted in the similar observations (Figure S6). We have also performed measurements with subsequent ligand washout, but those resulted in a slow Ca^{2+} run down and prolonged experiment time that might have an effect on cells (data not shown).

(K) Cartoon of the putative PHB-modification sites on the TRPM8 protein with a sequence indication for the extracellular PHBylated peptides targeted for the mutagenesis.

See also Figure S6.

chosen to replace the target residues, avoiding its replacement with hydrophobic residues that could attract the methyl groups on PHB.

Ca^{2+} measurements show that the activity of TRPM8 in both the double-serine mutant (S823G/S824G) and the quadruple-serine mutant (S819G/S820G/S823G/S824G) was altered insignificantly (Figures 2B, 2C, and 2J). On the other hand, the exchange of serine for glycine (S827G) at position 827 in the second peptide (SSLYSGRV 823–830) resulted in significant inhibition of TRPM8 responses to cold, menthol, and icilin (Figure 2F), suggesting that this serine may be involved in binding with PHB.

Introducing more conformational changes into the region by replacing the serine with proline resulted in further inhibition of channel activity in the mutants S819P/S820P, SSLYS-GGLYP (823–827), SSLYS-GGGGP (823–829), and S827P (Figures 2E, 2G, 2H, and 2I). A summary of the cold, menthol, and icilin responses of the serine mutants is presented in Figure 2J. Ca^{2+}-imaging measurements with application of cold or icilin alone were also performed (Figure S6). The amino acid sequence of the S3-S4 linker is shown in Figure S7.

As many mutants demonstrated significant alteration in channel function, we further evaluated whether the modified amino acids had an effect on the localization and expression of the channel. Both immunocytochemical analysis and biotinylation experiments demonstrated that the localization and the expression levels of the TRPM8 mutants have not been altered, and that the mutants are actively expressed in both plasma membrane and endoplasmic reticulum membranes, similarly to the wild-type TRPM8 (Figures S8 and S9).

Inhibition of TRPM8 by PHB-Depolymerase, PhaZ7, and Characteristics of the Hydrophobic Mutants

Alternatively, we studied TRPM8 activity in the presence of the PHB hydrolyzing enzyme, PHB-depolymerase, PhaZ7, a serine-hydrolase family enzyme that is naturally expressed in

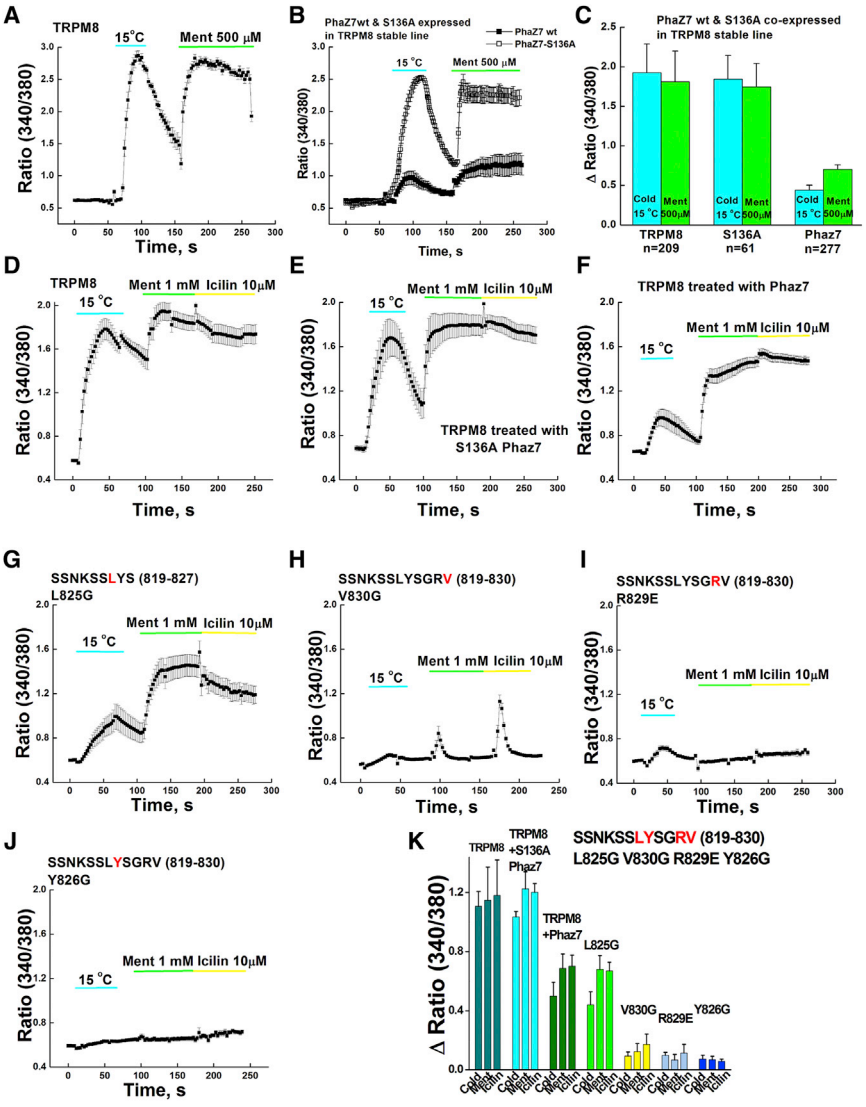

Figure 3. Inhibition of TRPM8 Activity by PHB-Depolymerase, PhaZ7, in Intracellular Ca^{2+} Measurements

(A–C) Fluorescence measurements of intracellular Ca^{2+} concentration were performed on HEK293 TRPM8 stable cell lines with transiently transfected either with GFP (0.2 μg) alone (n = 7; n_{cells} = 209) (A) or together with the PhaZ7 clone (0.7 μg) (n = 15; n_{cells} = 277) and the S136A-PhaZ7 mutant-inactive enzyme (0.7 μg) (n = 3; n_{cells} = 61) (B). The summaries of averaged cold and menthol responses with GFP-positive cells are represented in (C) ($p < 0.0005$; error bars stand for ± SEM).

(D–K) Fluorescence measurements of intracellular Ca^{2+} concentration were performed on HEK293 transiently transfected with TRPM8 (0.7 μg) and GFP (0.2 μg) (n = 7; n_{cells} = 71) (D). Further, TRPM8-expressing cells were treated for 1 hr with an inactive form of PHB-depolymerase, S136A PhaZ7 (n = 3; n_{cells} = 26) (E) and wild-type PhaZ7 (n = 3; n_{cells} = 40) (F). Ca^{2+} signals obtained from the HEK cells transiently expressing TRPM8 mutants: L825G (n = 5; n_{cells} = 83) (G), V830G (n = 6; n_{cells} = 90) (H), R829E (n = 5; n_{cells} = 39) (I), and Y826G (n = 5; n_{cells} = 37) (J). (A)–(J) are representative of single coverslips; the total number of measurements and the total number of cells for each variety are indicated in parentheses.

(K) The summaries of averaged cold, menthol, and icilin responses are represented (error bars stand for ± SEM).

the bacterium *Paucimonas lemoignei* (Kapetaniou et al., 2005; Reinhardt et al., 2002). We employed the PhaZ7 enzyme in two different applications. In one set of experiments, PhaZ7 was transiently expressed in a mammalian cell system, and in the other, the cells were treated with purified PhaZ7 protein to evaluate the activity of TRPM8.

Either the PhaZ7 protein or an inactive mutant of PhaZ7, S136A, subcloned into a mammalian vector was transiently coexpressed in human embryonic kidney 293 (HEK293) cells that stably expressed the TRPM8 channel. We found that the expression of PHB-depolymerase significantly inhibited both the cold- and the menthol-induced Ca^{2+}-signals (Figures 3A–3C), indicating that intracellular depletion of PHB associated with the TRPM8 protein affects TRPM8 channel function. Used as a control, S136A-PhaZ7 had no effect on the activity of TRPM8 (Figures 3A–3C).

Expression of the PhaZ7 protein and the S136A mutant was confirmed by western blot performed on cell lysates of HEK293 cells transiently expressing the proteins and also by immunocytochemistry experiments (Figures S10A and S10B). The activity of PhaZ7 expressed in HEK293 cells was confirmed by visualizing PHB levels with confocal microscopy, for which PHB was stained with Nile red (NR) (Figure S11A), the hydrophobic dye used to detect the polymer (Jendrossek et al., 2007; Pani et al., 2009; Tyo et al., 2006). In PhaZ7-expressing cells in particular, we found reduced NR signal in the plasma membrane regions, which confirms that depletion of PHB from the cytoplasm by the enzyme occurs in the vicinity of the plasma membrane (Figure S11B). Notably, NR signal was greater in the cells stably expressing TRPM8 channels (Figures S11A and S11B). PhaZ7 expression did not alter TRPM8 protein expression and localization, as indicated by immunocytochemistry experiments (data not shown). Treatment of the TRPM8 protein with the PhaZ7 enzyme in vitro reduced levels of PHB associated with TRPM8 upon cleavage in a time-dependent manner (Figure S11C).

Further, in order to focus on the PHB-modified peptide located on the external side of the channel, enzymatic treatment of PHB on the cell surface was performed. TRPM8-expressing cells were treated with the purified PhaZ7 protein (10 μg/ml) for 1 hr, and then the effect on Ca^{2+} transport was observed. A non-functional mutant of the enzyme, S136A-PhaZ7 (10 μg/ml), was used as a control. Ca^{2+} uptake through TRPM8 was notably

suppressed in cells treated with the active form of PHB-depolymerase (Figures 3F and 3K), which confirms the PHB modification of TRPM8 on the extracellular side of the channel and its importance for channel activity.

Next, we targeted a number of residues adjacent to serine. Due to the high hydrophobicity of PHB, altering hydrophobic interactions could have a strong impact on the function of the protein. Thus, a number of hydrophobic residues in the regions adjacent to serine were modified. The single mutation of leucine to glycine (L825G) inhibited TRPM8 activity in a manner kinetically very similar to that occurring after treatment with PHB-depolymerase (Figures 3F, 3G, and 3K). For example, the L825G mutation resulted in 60% inhibition of the cold-induced TRPM8 response, similar to the 54% inhibition after the PhaZ7 treatment. The L825G mutation also resulted in 40% and 42% inhibition of the menthol- and icilin-induced responses, respectively, similar to 42% inhibition of responses to either agonist observed in treated cells (Figure 3K). This pattern of similarity indicates that the externally located polyester that is being cleaved by the enzyme may reside in the vicinity of the hydrophobic interactions with the L825 residue.

Ca^{2+} uptake by the valine mutant (V830G) was severely inhibited with all the agonists tested (Figures 3H and 3K). In particular, this mutant exhibited 92% inhibition of the cold-induced TRPM8 response and 86% and 75% of the menthol- and icilin-induced responses, respectively (Figure 3K). The mutation of the hydrophobic residue tyrosine (Y826), located next to the possible PHB-binding serine 827, resulted in complete loss of channel function (Figures 3J and 3K).

We also considered participation of nonhydrophobic residues in the channel-polymer interaction. Mutation of the arginine at position 829 to glutamic acid (R829E) also had an immense effect on TRPM8 activity (Figures 3I and 3K). We suggest that such a dramatic change in TRPM8 channel behavior in the arginine mutant could be caused by a conformational change in this peptide. Notably, the putative S3-S4 linker (LHSSNKSSLYSGRV) comprises eight neutral, four hydrophobic, and three basic amino acids. It is possible that positively charged residues could repel each other to form a pocket-like structure, in which hydrophobic interactions between PHB methyl groups and hydrophobic amino acids take place. Replacing the positively charged arginine with the negatively charged glutamic acid might lead to ionic interactions in the region that could alter the structure of the pocket and prevent formation of the PHB-peptide complex, thus disrupting the function of the channel (Figure 3K).

Inhibition of TRPM8 Activity by PHB-Depolymerase in DRG Neurons

To detect PHB modification of TRPM8 in native cells, we further examined its role and association with TRPM8 expressed in rat dorsal-root ganglion (DRG) neurons. We found that transiently expressed PHB-depolymerase substantially suppressed TRPM8 activity in DRG neurons when induced by its usual agonists (Figures 4A, 4B, and 4D). We also transfected the neurons with the S827P mutant that had demonstrated low activity when expressed in HEK293 cells. Similar to its phenotype in HEK293 cells, there was not any notable Ca^{2+} uptake in DRG neurons in this mutant, suggesting that PHBylation of Ser827 also takes place in neurons (Figures 4C and 4D).

Next, we performed immunocytochemical examination of DRG neurons with anti-PHB antibodies. We found high-intensity signals for PHB in TRPM8-expressing neurons. Coexpression of PhaZ7 resulted in notable reduction of PHB signal, particularly in the regions of plasma membrane and neurites (Figure 4E).

Whole-Cell Patch Clamp Recordings of the PHB Mutants of TRPM8

PHB mutants of TRPM8 were also examined in whole-cell patch clamp recordings performed on HEK293 cells transiently expressing either the wild-type TRPM8 or mutant channels (Figure 5). The behavior of channels recorded by patch clamp paralleled that observed during Ca^{2+}-imaging experiments. In comparison to the wild-type TRPM8, the menthol-induced activity of the PHB mutants showed decreases in current density in the following order: S827G > L825G > 5S-G > S827p > V830G > Y826G (Figures 5A and 5C). Cold-induced activity of the mutants was more strongly inhibited and exhibited a similar order of inhibition: S827G > L825G > 5S-G > S827p > V830G > Y826G (Figures 5B and 5D).

Moreover, more detailed analysis of the cold dependence of the mutants demonstrated differences in relative activity upon stimulation with cold. Figure 5F demonstrates kinetics for the cold activation of wild-type TRPM8 compared with 5S-G, S827G, and L825G mutants. Lower current density was found for all of these mutants in comparison to that of wild-type (Figure 5F).

Planar Lipid Bilayer Experiments of PHB Mutants of TRPM8

Further, planar lipid bilayer experiments were performed to characterize the single-channel behavior of the mutants. Particularly, we focused here on the 5S-G mutant, which demonstrated distinct kinetics in patch clamp measurements. We also tested the mutants that exhibited the lowest activity in the patch clamp and Ca^{2+}-imaging experiments.

Figures 6A and 6B demonstrate representative recordings and a summary of the probabilities of a channel being open in the wild-type TRPM8 and in the mutants 5S-G, S827P, and Y826G (Figures 6A and 6B). We found that, in contrast to the wild-type channel ($P_o = 0.89 \pm 0.075$ at 100 mV), the 5S-G mutant activated with menthol operates in a different gating mode and exhibits a low open probability ($P_o = 0.211 \pm 0.174$ at 100 mV; n = 10; number of events analyzed = 11,019; Figures 6A and 6B). Furthermore, even fewer openings of the S827P mutant channel were observed with $P_o = 0.077 \pm 0.032$ at 100 mV (n = 6; number of events analyzed = 2,533). Subsequent addition of icilin to the bilayer did not alter the low open probability of the mutant (data not shown), indicating that the entire gating mechanism is affected. We could not detect any channel activity in the Y826G mutant, even when high amounts of the protein were added to the bilayer, thus confirming that the Y826G mutant is entirely inactive.

Next, we examined the responses of these mutants to cold activation. Cold-induced activity was detected only with the 5S-G mutant, while the S827P and the Y826G mutants were

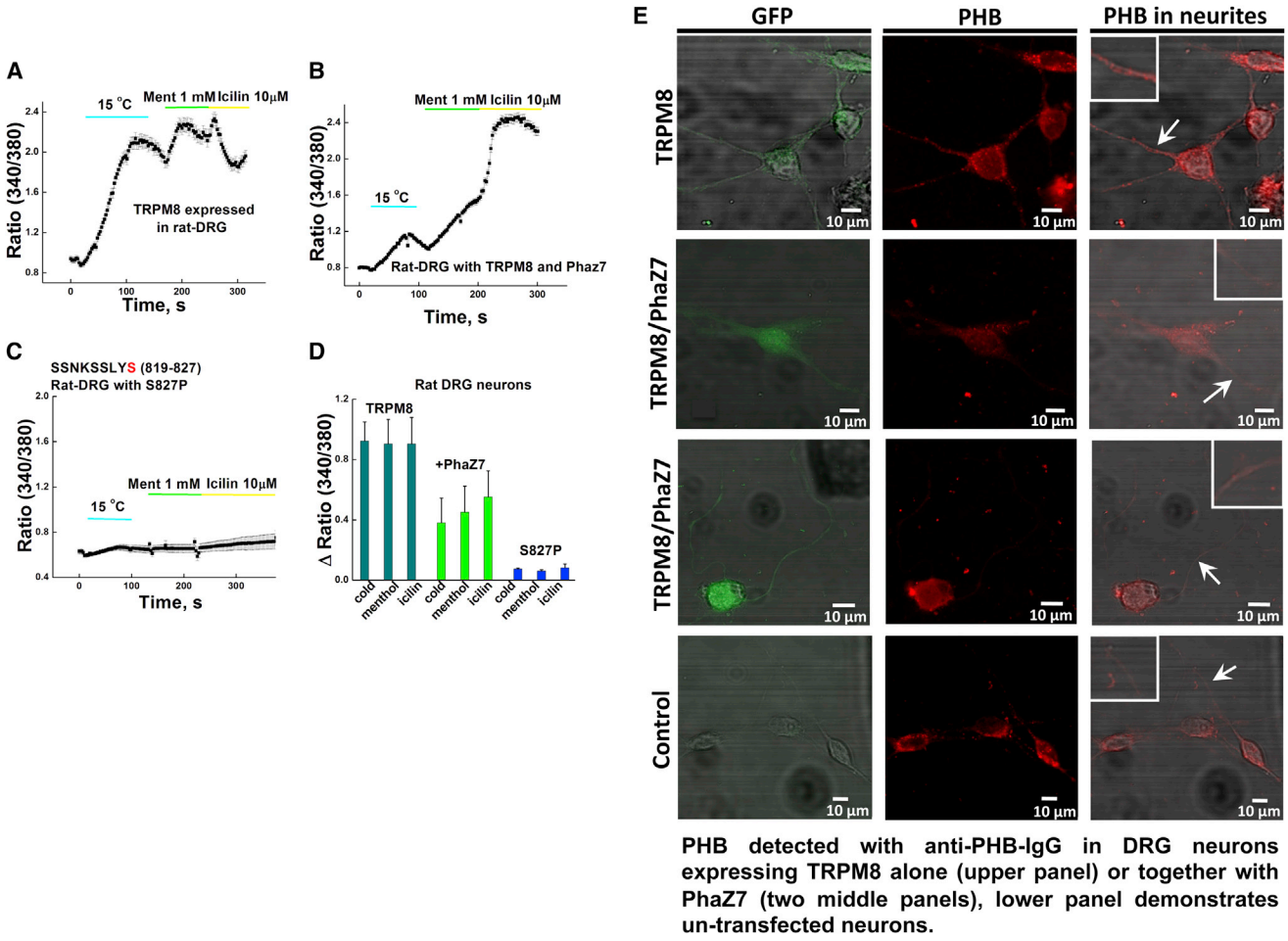

PHB detected with anti-PHB-IgG in DRG neurons expressing TRPM8 alone (upper panel) or together with PhaZ7 (two middle panels), lower panel demonstrates un-transfected neurons.

Figure 4. Inhibition of TRPM8 Activity by PHB-Depolymerase PhaZ7 in DRG Neurons

(A–C) Fluorescence measurements of intracellular Ca^{2+} concentration were performed on DRG neurons with transiently transfected TRPM8 (3 μg) and GFP (0.5 μg) (n = 4; $_{cells}$ = 7) (A), TRPM8 together with the PhaZ7 clone (3 μg) (n = 5; n $_{cells}$ = 10) (B), and mutant S827P (3 μg) (n = 3; n $_{cells}$ = 6) (C). (A)–(C) are representatives of single coverslips; total number of experiments and number of neurons are indicated in parentheses.

(D) The summaries of averaged cold and menthol responses are represented (error bars stand for ± SEM). Details of the neuronal transfection are given in Extended Experimental Procedures.

(E) PHB signals enhanced in DRG neurons expressing TRPM8. DRG neurons expressing TRPM8/GFP or TRPM8/PhaZ7/GFP were immunoprobed with anti-PHB-IgG and Alexa-546 (red) as secondary antibodies. The transfection conditions are the same as described for (A) and (B). PHB-depolymerase hydrolyzes PHB, which results in reduced signals from plasma membrane and neurites. The upper panel shows PHB staining in DRG neurons transiently expressing TRPM8 and GFP; the two middle panels demonstrate PHB in neurons expressing TRPM8, PhaZ7, and GFP; and the lower panel shows PHB in untransfected neurons. For immunocytochemical analysis, cells were observed with a Zeiss LSM-510 confocal microscope (60X objective) equipped with an Argon laser (488 nm), a red diode laser (637 nm), and a green HeNe laser (543 nm), in the Confocal Imaging Facility of the New Jersey Medical School.

not active, even when temperature of the bilayer was reduced to 3°C. Representative current traces of the 5S-G mutant activated by cold and the change in its open probability over a range of temperatures (n = 11; number of events analyzed = 5,535) are shown in Figures 6C and 6D. The 5S-G mutant exhibited a substantial ~5°C shift in activation temperature (~13°C) for its maximum open probability, relative to that of wild-type TRPM8 (~18°C; Figure 6D). The mutant also exhibited different activation kinetics from those of wild-type TRPM8. Thermodynamic analysis of the 5S-G mutant demonstrated that the mutant is less temperature sensitive than the wild-type TRPM8 and exhibits a single-phase transition for channel opening during cold activation compared to the two-phase activation of wild-type TRPM8 (Brauchi et al., 2004; Zakharian et al., 2010). Both enthalpy and entropy changes are reduced to a single-phase activation for the 5S-G mutant with $\Delta H = -519.2$ kJ/mol and $\Delta S = -1.794$ kJ/molK (Q_{10} = 23), respectively. Enthalpy and entropy values for wild-type TRPM8 with dual transitions for channel gating were $\Delta H = -792.8$ kJ/mol and $\Delta S = -2.716$ kJ/molK (Q_{10} = 40), respectively, for the first phase and $\Delta H = -262.2$ kJ/mol and $\Delta S = -0.886$ kJ/molK (Q_{10} = 1.6), respectively, for the second phase (Zakharian et al., 2010). Decline in both enthalpy change (lessen by −273.6 kJ/mol) and entropy change (lessen

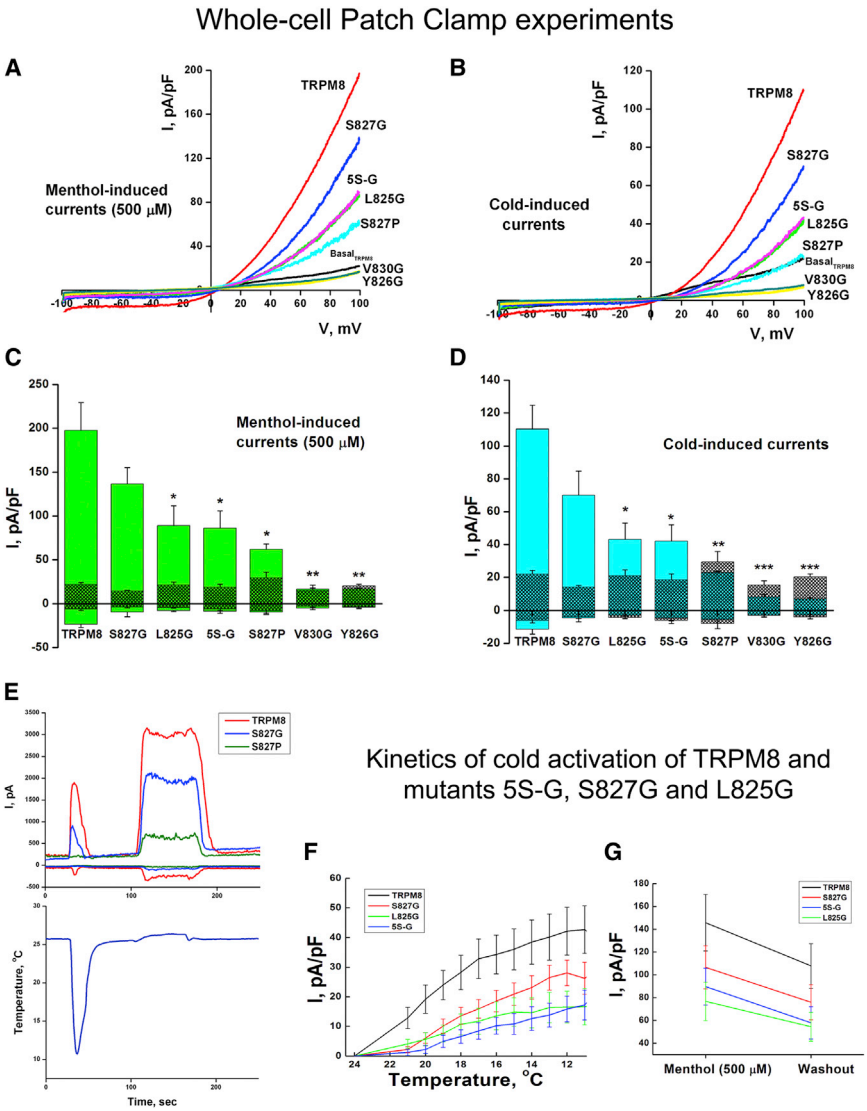

Figure 5. Electrophysiological Characterization of TRPM8 and Other Mutants' Sensitivity to Menthol and Cold Stimulus

Whole-cell current-voltage relationships from voltage ramps (−100 +100 mV) were obtained for HEK293 cells expressing the wild-type TRPM8 (n = 7) and the mutant channels: 5S-G (n = 5); S827G (n = 4); S827P (n = 4); L825G (n = 4); Y826G (n = 3); and V830G (n = 4); measurements were performed in the presence of 2 mM Ca^{2+}.

(A) Averaged ramp recordings for menthol-induced currents (500 μM).

(B) Cold-induced currents (10°C). Control values for background current for the wild-type TRPM8 and mutants are very close, and only background wild-type TRPM8 current was demonstrated.

(C and D) Summary of the menthol-induced whole-cell currents at −100 and +100 mV potentials are shown in (C) and those for cold-induced currents in (D). For each group, background current marked in gray color.

(E) Representative current traces for −100 + 100 mV potentials of the cold-induced and subsequent menthol-induced currents obtained for the wild-type TRPM8 and single mutants, S827G and S827P. In comparison to the wild-type TRPM8, the menthol-induced activity of the PHB mutants showed a reduction in current density in the following sequence S827G (p = 0.212 at +100 mV; p = 0.0465 at −100 mV) > L825G (p = 0.044 at 100 mV; p = 0.0097 at −100 mV) > 5S-G (p = 0.023 at +100 mV; p = 0.0088 at −100 mV) > S827P (p = 0.012 at +100 mV; p = 0.024 at −100 mV) > V830G (p = 0.0024 at +100 mV; p = 0.0041 at −100 mV) > Y826G (p = 0.0072 at +100 mV; p = 0.0085 at −100 mV) (A and C). The cold-induced activity of the mutants was inhibited to a greater degree and exhibited a similar pattern of inhibition: S827G (p = 0.105 at +100 mV; p = 0.141 at −100 mV) > L825G (p = 0.0106 at 100 mV; p = 0.0559 at −100 mV) > 5S-G (p = 0.0054 at +100 mV; p = 0.096 at −100 mV) > S827P (p = 0.0016 at +100 mV; p = 0.186 at −100 mV) > V830G (p = 0.00005 at +100 mV; p = 0.0569 at −100 mV) > Y826G (p = 0.002 at +100 mV; p = 0.092 at −100 mV) (B and D). The number of asterisks in the graphs indicates the significance level: one (*) for $p \leq 0.05$, two (**) for ≤ 0.01, and three (***) for ≤ 0.001.

(F and G) Kinetics of cold activation of TRPM8 and mutants 5S-G, S827G, and L825G and their menthol-induced desensitization. Summary plot of experiments showing cold ramp (drop to 10°C in 15 s) (F) and menthol-induced (G) whole-cell currents for the wild-type TRPM8 (n = 10) and mutants 5G (n = 5), S827G (n = 9), and L825G (n = 8) at +100 mV potentials. To minimize current desensitization, this set of experiments was performed in Ca^{2+}-free extracellular solution. (G) demonstrates slight but nonsignificant current desensitization for all three experimental replications of menthol application. All error bars stand for ± SEM.

by −0.922 kJ/molK) indicates that temperature sensitivity of the 5S-G mutant is substantially decreased.

PHB Modification in the Y826G and the 5S-G Mutants

Functional analysis indicated that 5S-G exhibits distinct kinetics and less sensitivity to cold activation in addition to altered gating of the menthol-activated currents, while Y826G has no activity. In order to understand the alteration of TRPM8 activity in these mutants, further experiments were performed to detect PHB in 5S-G and Y826G.

We first attempted to identify differences in PHB levels of the entire TRPM8 protein by western blot analyses (Figure S12). However, no differences were found between the wild-type TRPM8 and the 5S-G and Y826G mutants, which might be due to high-intensity signal from the intracellular PHBylated peptides. Next, immunocytochemical analyses of nonpermeabilized cells were conducted and the extracellular PHB levels of the 5S-G mutant were found to be significantly reduced in comparison to wild-type TRPM8, while the Y826G mutant contained no PHB (Figures 7A and 7B). The expression of the protein at the cell surface was not altered (Figures 7C and 7D).

As for the western blot results (Figure S12), when the entire protein/PHB complex was stained under permeabilized conditions, no difference in PHB labeling between the mutants and

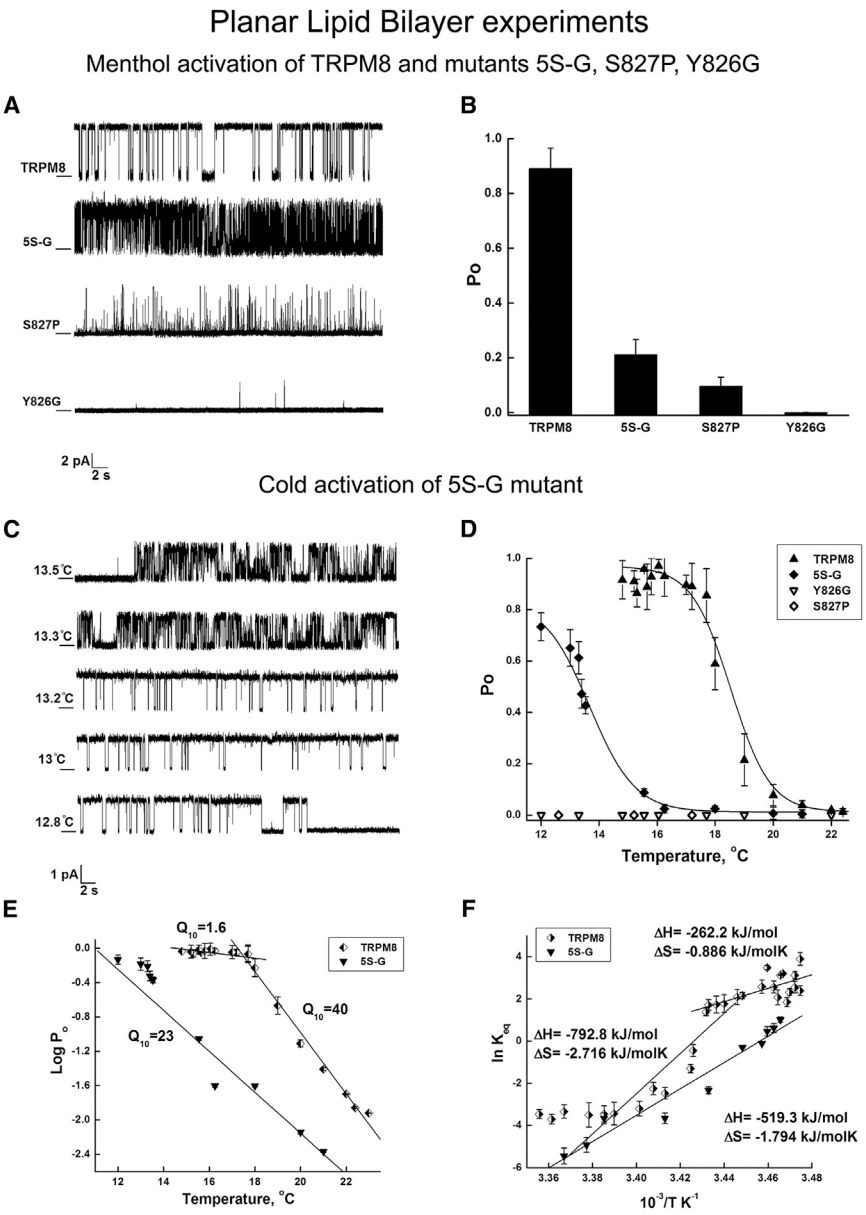

Figure 6. Menthol-Induced Activity of Wild-Type TRPM8 and 5S-G, S827P, and Y826G Mutant Channels in the Planar Lipid Bilayers

Representative single-channel current recordings of TRPM8 and the mutant channels incorporated in planar lipid bilayers formed from 1-palmitoyl-2-oleoyl-glycero-3-phosphocoline (POPC)/1-palmitoyl-2-oleoyl-glycero-3-phosphoethanolaminein (POPE) (3:1) in *n*-decane between symmetric bathing solutions of 150 mM KCl, 0.2 mM $MgCl_2$ in 20 mM 4-(2-hydroxyethyl)-1-piperazineethanesulfonic acid buffer, pH 7.4 at 22°C. Between 0.2 and 0.5 μl of 0.2 μg/ml, the protein was incorporated into POPC/POPE micelles and added to the cis compartment (ground). Clamping potential was +100 mV. The closed state is delineated by a horizontal line under the traces on the left.

(A) Representative currents traces in the presence of 4 μM of DiC_8 PtdIns(4,5)P_2 and 500 μM of menthol.

(B) Open probabilities of the wild-type (WT) TRPM8 and mutants obtained at +100 mV.

(C) Cold activation of 5S-G mutant channels in planar lipid bilayer and P_o change for the wild-type TRPM8 and mutants. Representative single-channel current recordings of 5S-G mutant channels activated by cold in the presence of 4 μM diC_8PIP_2. Clamping potential was +100 mV.

(D) Open probability for the wild-type TRPM8 and 5S-G mutant obtained during cooling the planar lipid bilayers.

(E) Two-phase TRPM8 temperature dependence and single-phase of 5S-G mutant in log(P_o) versus T plot.

(F) Van't Hoff plot of the equilibrium constant K_{eq} demonstrates two-phase channel transitions for wild-type TRPM8 and a single transition obtained for 5S-G mutant. Changes in enthalpy and entropy of TRPM8 and 5S-G activation are indicated on the graph. All error bars stand for ± SEM.

the wild-type was detected, most likely due to the strong staining signals from the intracellular PHBylation sites (data not shown).

We also performed MS analysis of the chloroform extracts of the S827G, Y826G, and 5S-G mutants (Figure S13). We found neither PHB modification of the target peptides nor peaks in chloroform fractions corresponding to the parental peptides of these mutants, suggesting that, unlike the wild-type TRPM8, in which we see a very strong peak for the parental peptide, without PHB, the mutant peptides cannot enter the chloroform fraction (Figures 1 and S4). Although we have removed the ability of the 5S-G and S827G mutant peptides to covalently bind to PHB (Figures S13A and S13C), we suggest that the PHB polymer is still present at low levels, due to its attraction to the hydrophobic residues on the native protein, as indicated by PHB staining on the cell surface (Figures 7A and 7B). Our model suggests that the hydrophobic interaction of PHB with the hydrophobic residues bring it into proximity with the extracellular S3-S4 linker and that this interaction ensures the covalent binding of the polymer to serine and formation of the PHB-TRPM8 complex (Figure 7E).

DISCUSSION

TRP channels play important roles in the perception of the environment. They respond to a number of physical and chemical stimuli and demonstrate an unusual complexity of regulatory modes. TRPM8 is a representative member of this channel family and exhibits a broad variety of functional modes with a number of allosteric regulators (Latorre et al., 2011; Yudin and Rohacs, 2012).

TRPM8 is regulated by a number of environmental factors. The TRPM8 channel is activated in a mild temperature range of 10°C–28°C (McKemy et al., 2002; Peier et al., 2002), by chemical

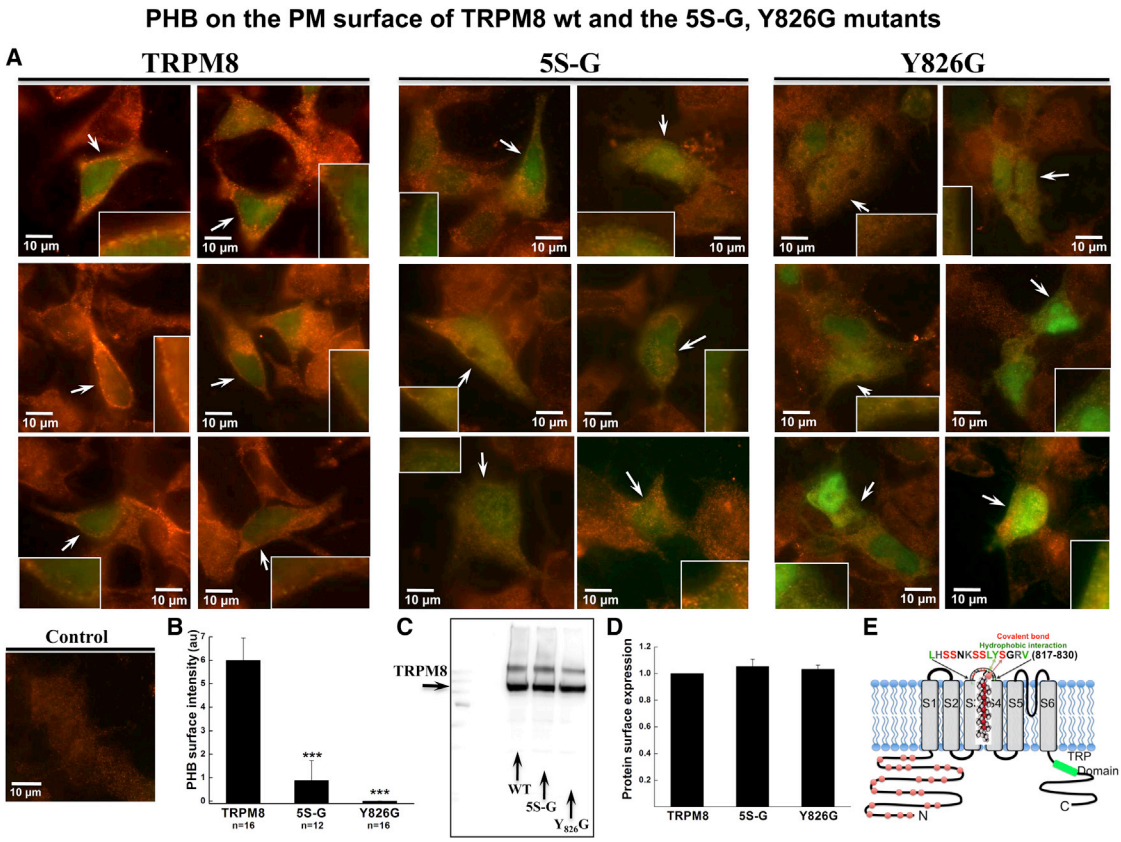

Figure 7. Extracellular PHB Levels of Cells Expressing the 5S-G and Y826G Mutants Are Significantly Reduced

(A) PHB signals on the cell surface obtained by immunocytochemical analysis of the polymer with anti-PHB-IgG on nonpermeabilized cells detected with confocal microscopy (for details, see Extended Experimental Procedures). The images were obtained with a Zeiss LSM-510 confocal microscope (60X objective). HEK293 cells were transiently transfected with the wild-type TRPM8 (1 μg), the 5S-G (1 μg), and the Y826G (1 μg) mutants along with GFP (0.2 μg) for detection purposes.

(B) Summary of intensities of the PHB signals on the surface of plasma membrane measured for the wild-type TRPM8 and the mutants 5S-G and Y826G.

(C) The surface expression of the protein is not altered (all error bars stand for ± SEM). The wild-type TRPM8 and the mutants (5S-G, Y826G) were biotinylated and captured with streptavidin beads as described under the Extended Experimental Procedures.

(D) Arithmetic means of the relative density of the proteins in the membrane fraction of the wild-type TRPM8 and the 5S-G and Y826G mutants, n = 3.

(E) Cartoon of a model for the PHB-TRPM8 complex with PHB attachment to the extracellular peptide LHSSNHSSLYSGR (817–829) and supported by a covalent bond to S827 and by hydrophobic interactions with Y826 and other hydrophobic residues in the region; red spheres show putative intracellular PHBylation sites of TRPM8.

agonists such as menthol, eucalyptol, and icilin (Chuang et al., 2004; McKemy et al., 2002; Peier et al., 2002), and by depolarizing voltages (Brauchi et al., 2004; Nilius et al., 2007; Voets et al., 2004). The channel also requires phosphatidylinositol-(4,5)-bisphosphate (PIP_2), the primary gating factor for TRPM8 (Liu and Qin, 2005; Rohács et al., 2005; Yudin et al., 2011; Zakharian et al., 2009, 2010). Posttranslational modifications, such as N-glycosylation, have been shown to affect the function of native TRPM8 ion channels (Pertusa et al., 2012). Lipid raft association was also shown to modulate TRPM8 channel activity, and interestingly, such compartmentalization is preferred by the N-glycosylated species of the channel (Morenilla-Palao et al., 2009).

The versatility of TRPM8 is also apparent at the level of molecular organization. Recently, we demonstrated that the functional TRPM8 channel exists as a complex with inorganic polyphosphate (polyP). PolyP is associated with the TRPM8 protein via ionic interactions, and it plays a role in the gating of the channel (Zakharian et al., 2009). We suggested that the presence of polyP might be supported by another homopolymer—poly-(R)-3-hydroxybutyrate—PHB. Here, we aimed to identify PHB-modification sites on the TRPM8 protein and determine the role of PHB in TRPM8 channel function.

In bacteria, specific enzymes, known as PHB synthases, assemble PHB from CoA esters of R-3-hydroxybutyrate. The enzymes for the synthesis of PHB in eukaryotes are as yet unknown. However, the metabolites that are involved in PHB production in bacteria are also present in eukaryotes, and it is possible that similar metabolic pathways for this polymer operate in both prokaryotes and eukaryotes. Likewise, not much is known regarding enzyme(s) that hydrolyze PHB in eukaryotic cells. Even in bacteria, these enzymes are not conserved among various species. For example, the recently discovered bacterial

PHB-depolymerase, PhaZ7, is not a conventional esterase or lipase (Handrick et al., 2001). According to its biochemical properties, PhaZ7 represents the first member of a new subgroup (EC 3.1.1.75) of serine hydrolases with no significant amino acid similarities to any other PHB-depolymerases, lipases, or hydrolases apart from a lipase-box structure comprised of Ala-His-Ser_{136}-Met-Gly (Kapetaniou et al., 2005; Papageorgiou et al., 2008).

Furthermore, not much is known regarding the role of PHB in eukaryotic cells. We also observe PHB both in DRG neurons and HEK293 cells that are not expressing TRPM8 channel (Figures 4E, lower panel, S10B, S11A, and S11B). However, the other molecules or organelles to which the polymer may be related and the role it may play are unknown.

In this study, we found that PHB covalently binds to the TRPM8 protein, possibly via its CoA-ester end by formation of an ester bond. The high-energy CoA group could be an important cofactor for the PHBylation enzymatic reaction, analogous to that for other posttranslational modifications, such as acylation, acetylation, propionylation, and butyrylation (Chen et al., 2007; Mukherjee et al., 2007). Recently, succinyl-CoA has also been proposed to function as a cofactor for enzyme-mediated lysine succinylation (Zhang et al., 2011).

Evidence for PHBylated peptides was derived from the MS/MS spectrum of a large quadruply charged precursor ion (Figure 1E). De novo assignment of posttranslational modifications is very challenging under these circumstances, due to technical limitations, such as the limited mass range, and the complexity of the fragmentation routes generated by multiple charged species. However, together with the rest of the evidence presented, a modification causing a mass shift of the magnitude compatible with two PHB units would be consistent with the presence of polyester moieties on this peptide.

The MS analysis of the aqueous fraction of trypsin-digested TRPM8 was also confirmed for the chloroform-extracted peptides (Figures 1, S2, S3, S4, S5, and S6). PHB is highly soluble in chloroform but weakly soluble in less hydrophobic organic solvents, such as methanol, ethanol, ethyl acetate, acetone, and other common organic media, and is insoluble in water (Seebach and Fritz, 1999). The strong hydrophobicity of PHB is responsible for its ability to carry even highly charged molecules, such as polyP and Ca^{2+}, into the chloroform fraction (Seebach et al., 1994; Seebach and Fritz, 1999). The reason for high hydrophobicity of the amphiphilic in its chemical structure, PHB, is due to its molecular arrangement: the ester oxygens of the polymer are constrained toward the inside of the helix, while its methyl groups extend outward, covering the polymer with an entirely lipophilic surface (Seebach and Fritz, 1999). Even short oligomers of PHB are water insoluble. Therefore, attachment of water-insoluble PHB to an otherwise hydrophilic peptide makes that peptide less water soluble and more lipid soluble.

The MS analysis shows that PHB is conjugated to a large number of TRPM8 peptides (Figures S2 and S3). The role of this modification has not been established, as only a handful of studies have been performed on the bacterial proteins (Negoda et al., 2010; Xian et al., 2007). In this study, using site-directed mutagenesis, we created several mutations in one of the PHB-binding peptides and determined how these mutations affect TRPM8 channel function. This modified extracellular domain lies in the region of the putative S3-S4 linker where PHB may be attached to one or more serine residues in the amino acid sequence LHSSNKSSLYSGRV (817–830) (Figures 1 and S4). We suggest that the hydroxyl group of serine is important for PHB modification and makes the serine residue suitable for the formation of the covalent ester bond to the polyester. For the same reason, threonine may also be suitable for PHB modification. However, previous observations indicated that PHB modifications occur on serine residues and hydrophobic residues supporting these interactions.

The PHB-modified peptides detected by the MS analysis in our data are similar in composition to those of the known PHB-conjugated proteins. For example, in the potassium channel KcsA from *S. lividans*, PHB is covalently bound to serines (S102 and S129), and mutation of these residues significantly alters the channel activity (Negoda et al., 2010). In the bacterial outer membrane protein A (OmpA) of *E. coli*, PHB is covalently bound to serines (S163 and S167), and this binding is secured by hydrophobic interactions with valine and leucine (Xian et al., 2007). It is noteworthy that PHB-depolymerase, PhaZ7, is a serine hydrolase with Ser136 as the central amino acid in the catalytic triad, and a single mutation of this serine completely inactivates the enzyme (Braaz et al., 2003). However, the binding of PhaZ7 to its substrate, PHB, is mediated by hydrophobic residues, such as Tyr105, so mutation of this amino acid significantly reduces the ability of the enzyme to bind PHB for hydrolysis (Hermawan and Jendrossek, 2010). Analogously, here, PHB is recruited by the hydrophobic residues to the 5S-G mutant peptide, which helps retain this mutant function (Figures 2, 5, 6, and 7A), without the formation of a covalent bond (Figures S13A and S13C). However, both the gating and the temperature sensitivity of this mutant channel are suppressed by the lack of PHB covalently anchored to serine. On the other hand, the hydrophobic mutant Y826G has no PHB at all bound to the peptide (Figures 7A, 7B, and S13B), which might be the reason for its complete loss of channel activity (Figures 3, 5, and 6). These results suggest that the extracellular PHB modification is required for the TRPM8 channel function. However, we cannot rule out a possibility that the Y826 residue alone is critical for TRPM8 function, and PHB is not an absolute requirement for the channel activity.

Interestingly, the serine mutant shows only an alteration in channel gating, while the hydrophobic residue mutations have a stronger effect. We suggest that the residual activity of the serine mutant derives from the small portion of TRPM8 that still contains PHB attracted by the hydrophobic residues in the region (Figure 7). Because it is no longer covalently bound, we are not able to detect PHB on the serine mutant during MS experiments (Figure S13). This does not mean that serine is less specific, it is rather only one of several binding residues, and it seems that, in case of PHB, a covalent bond is not more important than hydrophobic interactions. The relative importance for the protein-PHB complex of both the covalent bonds and hydrophobic interactions is a central question. Our insights into this complex issue are limited by available methodology. Nevertheless, it is apparent that the binding of this massive polymer should be supported by many residues and noncovalent

bonds and that those bonds participate further in the functional interactions and conformational dynamics of the molecular complex. Unlike the other posttranslation modifications, such as phosphorylation or glycosylation, protein modification by PHB has to be engaged with several residues; therefore, there is a greater network in the interactions.

PHB-binding mutants in the S3-S4 linker of TRPM8 demonstrated deficient channel responses to all agonists tested (Figures 2 and 5), although the response to cold was more negatively affected. Interestingly, the polyester is involved in regulation of TRPM8 via all of its allosteric agonists. Participation of PHB in the transduction of the cold stimulus to opening of the channel is perhaps most predictable, due to the high flexibility and total conformational energy of the polymer. In polysaccharides and polypeptides, total conformational energy generally is a function of two dihedral angles; however, the PHB molecule is even more complicated because there are four dihedral angles in the residue instead of two and, additionally, a small deviation from planarity of the ester groups (Cornibert and Marchessault, 1972). This flexibility and conformational energy of the polymer may explain the very large enthalpy and entropy changes for the gating of TRPM8. The hydrophobicity of PHB also agrees well with the thermodynamic profile of TRPM8. Perspectives recently presented by D. Clapham and C. Miller for temperature-sensitive TRP channels introduced a theoretical postulate for the involvement of a large number of hydrophobic groups in the conformational changes of TRP channels during temperature activation (Clapham and Miller, 2011). Our data indicate that there are approximately 26 PHB units per peptide, which is sufficient to form a polymer with a length of about 48 Å when fully extended (Seebach and Fritz, 1999). This indicates that the bulk chain of the polyester might be introduced into a large region of the protein and therefore could induce the large net of conformational changes upon channel activation.

One possible scenario is that the PHB polyester stiffens or contracts with lower temperatures (glass temperature of PHB is ~10°C). This contraction of the polymer would have a strong conformational impact upon the protein, due to its multiple PHB-interacting sites, including covalent bonds, various hydrophobic bonds with the methyl groups, hydrogen, and coordinate bonds. Considering the presence of 26 units of PHB would provide at least ~26 interacting sites in just one peptide region. Thus, as PHB changes its conformation, it could exert tension on the surrounding amino acids, resulting in massive conformational changes along the protein followed by channel openings. Notably, the bacterial PHBylated proteins, OmpA and KcsA, are both temperature-sensitive and undergo significant temperature-dependent rearrangements (Zakharian and Reusch, 2004, 2005).

Menthol and icilin activate TRPM8 via a number of different amino acids. The menthol-binding hydrophobic residue Y745 is located in the S2 domain, whereas Y1005 and L1009 are located in the TRP domain at the C terminus of TRPM8 (Bandell et al., 2006). The icilin-binding site is located in the S2-S3 linker, where it sensitizes TRPM8 by acting through amino acid residues N799, D802, and G805 (Chuang et al., 2004). Both of these agonists act on the channel allosterically; however, our results indicate that removing PHB-modification sites most likely affects the entire network of conformational changes in TRPM8 that are involved in the general transition of channel openings.

The amino acid sequence of the S3-S4 linker of TRPM8 is not conserved in other TRPM channels but is entirely conserved in TRPM8 among different species (Figures 1E and S7). This suggests that the extracellular PHB modification is unique to the cold receptor. On the other hand, the N terminus is conserved among all known TRPM channels and is not homologous to other proteins. It is possible that PHB modifications of the N terminus observed here are also common to the other TRPM family members. It is noteworthy that one of the candidate peptides that was detected in the present study by LC-MS/MS (amino acid sequence AMESICKCGYAQSQHIEGTQINQNEK [63–88]; Figures 1E and 1F) is located within the N-terminal region that is essential for the formation of functional TRPM8 channels (Phelps and Gaudet, 2007). Furthermore, the specificity of PHBylation for cold receptors, heat receptors, or nontemperature-sensitive channels is not clear, and further studies are needed to understand the role of this modification.

In summary, our data suggest that PHB has an essential role in the structure and function of the TRPM8 channel protein and may participate in the stimulus-induced network of conformational changes that result in opening of the channel.

EXPERIMENTAL PROCEDURES

For detailed methods see the Extended Experimental Procedures.

Cell Culture

HEK293 cells were maintained in minimal essential medium (MEM), as previously described (Zakharian et al., 2009). Rat DRG neurons were purchased from Lonza and cultured in primary neuron basal medium (PNBM).

Whole-Cell Patch Clamp Recordings

The whole-cell patch clamp experiments for cold-induced and menthol-induced TRPM8 activity were performed as previously described (Yudin et al., 2011; Zakharian et al., 2009).

Intracellular Ca^{2+} Measurements

Ca^{2+} measurements were performed as previously described (Zakharian et al., 2009).

Preparation of the TRPM8 Protein from HEK Cells

TRPM8 protein isolation was performed as previously described (Zakharian et al., 2010). TRPM8 was purified by immunoprecipitation with anti-Myc-immunoglobulin G (IgG) conjugated to A/G protein magnetic beads (Pierce, Thermo Scientific). For the planar lipid bilayer experiments, the protein was eluted with Myc-peptide (50 μg/ml), and for mass-spectral analysis, protein samples were boiled in SDS sample buffer to harvest maximal amounts of the protein.

Mass Spectrometry

The proteins were separated on a SDS-PAGE gel (Figure S14). The gel band at a molecular weight corresponding to TRPM8 was excised for in-gel trypsin digestion with dithiothreitol (DTT) reduction and iodoacetamide alkylation (Selvamurugan et al., 2009). The resulting peptides were partitioned against $CHCl_3$ (in 1:1 ratio). The $CHCl_3$ fraction was concentrated in a centrifugal evaporator (SpeedVac, Savant) and subjected to analysis on either a 4800 MALDI time of flight (TOF)/TOF instrument (ABSciex) or an Orbitrap Velos tandem mass spectrometry instrument (Thermo Fisher Scientific) coupled with an Ultimate 300 Nano HPLC (Dionex, Thermo Fisher Scientific).

Planar Lipid Bilayer Measurements

Planar lipid bilayer measurements and temperature studies were performed as previously described (Zakharian et al., 2010).

Immunocytochemistry and Fluorescence Microscopy

All cell images were obtained using a confocal microscope. Immunocytochemistry experiments were performed as previously described (Zakharian et al., 2009). The details of the method and various conditions are described in Extended Experimental Procedures.

For Nile red staining, the cells were incubated with 0.3 μM NR (Nile red [9-diethylamino-5H-benzo[α]phenoxazine-5-one], Sigma) in PBS buffer for 5 min. The images were observed with 457 nm excitation to reduce the signal from polar lipid content and with 535 nm emission filters (Pani et al., 2009).

SUPPLEMENTAL INFORMATION

Supplemental Information includes Extended Experimental Procedures and 14 figures and can be found with this article online at http://dx.doi.org/10.1016/j.celrep.2013.06.022.

ACKNOWLEDGMENTS

We would like to acknowledge the work of Dr. Rosseta Reusch as a pioneer in the field of protein/PHB complexes and thank her for the inspiration for these studies as well as for providing us with the antibodies against PHB. We are thankful to Dr. Robert Winkfein for providing us with the mammalian clone of PHB-depolymerase, PhaZ7. This work was supported by American Heart Association grant SDG-2640223 (to E.Z.) and National Institutes of Health grants R01GM098052 (to E.Z.) and NS055159 (to T.R.). The authors are grateful for funding support from NIH grant NS046593 (to H.L.) and the continued support of the NINDS NeuroProteomics Core Facility at UMDNJ, New Jersey Medical School. C.C., Y.Y., Y.B., W.C., and T.L. performed experiments and analyzed data; H.L. and T.R. edited the paper; A.C. provided technical advice and help with the MS data analysis; D.J. provided *phaZ7* clones and PhaZ7 antiserum and edited the paper; E.P. gave technical support and conceptual advice and edited the paper; and E.Z. developed the concept, designed and performed experiments, analyzed data, and wrote the paper.

Received: January 14, 2013
Revised: April 1, 2013
Accepted: June 18, 2013
Published: July 11, 2013

REFERENCES

Bandell, M., Dubin, A.E., Petrus, M.J., Orth, A., Mathur, J., Hwang, S.W., and Patapoutian, A. (2006). High-throughput random mutagenesis screen reveals TRPM8 residues specifically required for activation by menthol. Nat. Neurosci. *9*, 493–500.

Bautista, D.M., Siemens, J., Glazer, J.M., Tsuruda, P.R., Basbaum, A.I., Stucky, C.L., Jordt, S.-E., and Julius, D. (2007). The menthol receptor TRPM8 is the principal detector of environmental cold. Nature *448*, 204–208.

Behrendt, H.J., Germann, T., Gillen, C., Hatt, H., and Jostock, R. (2004). Characterization of the mouse cold-menthol receptor TRPM8 and vanilloid receptor type-1 VR1 using a fluorometric imaging plate reader (FLIPR) assay. Br. J. Pharmacol. *141*, 737–745.

Braaz, R., Handrick, R., and Jendrossek, D. (2003). Identification and characterisation of the catalytic triad of the alkaliphilic thermotolerant PHA depolymerase PhaZ7 of Paucimonas lemoignei. FEMS Microbiol. Lett. *224*, 107–112.

Brauchi, S., Orio, P., and Latorre, R. (2004). Clues to understanding cold sensation: thermodynamics and electrophysiological analysis of the cold receptor TRPM8. Proc. Natl. Acad. Sci. USA *101*, 15494–15499.

Castuma, C.E., Huang, R., Kornberg, A., and Reusch, R.N. (1995). Inorganic polyphosphates in the acquisition of competence in Escherichia coli. J. Biol. Chem. *270*, 12980–12983.

Chen, Y., Sprung, R., Tang, Y., Ball, H., Sangras, B., Kim, S.C., Falck, J.R., Peng, J., Gu, W., and Zhao, Y. (2007). Lysine propionylation and butyrylation are novel post-translational modifications in histones. Mol. Cell. Proteomics *6*, 812–819.

Chuang, H.H., Neuhausser, W.M., and Julius, D. (2004). The super-cooling agent icilin reveals a mechanism of coincidence detection by a temperature-sensitive TRP channel. Neuron *43*, 859–869.

Clapham, D.E., and Miller, C. (2011). A thermodynamic framework for understanding temperature sensing by transient receptor potential (TRP) channels. Proc. Natl. Acad. Sci. USA *108*, 19492–19497.

Colburn, R.W., Lubin, M.L., Stone, D.J., Jr., Wang, Y., Lawrence, D., D'Andrea, M.R., Brandt, M.R., Liu, Y., Flores, C.M., and Qin, N. (2007). Attenuated cold sensitivity in TRPM8 null mice. Neuron *54*, 379–386.

Cornibert, J., and Marchessault, R.H. (1972). Physical properties of poly- -hydroxybutyrate. IV. Conformational analysis and crystalline structure. J. Mol. Biol. *71*, 735–756.

Dhaka, A., Murray, A.N., Mathur, J., Earley, T.J., Petrus, M.J., and Patapoutian, A. (2007). TRPM8 is required for cold sensation in mice. Neuron *54*, 371–378.

Handrick, R., Reinhardt, S., Focarete, M.L., Scandola, M., Adamus, G., Kowalczuk, M., and Jendrossek, D. (2001). A new type of thermoalkalophilic hydrolase of Paucimonas lemoignei with high specificity for amorphous polyesters of short chain-length hydroxyalkanoic acids. J. Biol. Chem. *276*, 36215–36224.

Hermawan, S., and Jendrossek, D. (2010). Tyrosine 105 of Paucimonas lemoignei PHB depolymerase PhaZ7 is essential for polymer binding. Polym. Degrad. Stabil. *95*, 1429–1435.

Jendrossek, D., Selchow, O., and Hoppert, M. (2007). Poly(3-hydroxybutyrate) granules at the early stages of formation are localized close to the cytoplasmic membrane in Caryophanon latum. Appl. Environ. Microbiol. *73*, 586–593.

Kapetaniou, E.G., Braaz, R., Jendrossek, D., and Papageorgiou, A.C. (2005). Crystallization and preliminary X-ray analysis of a novel thermoalkalophilic poly(3-hydroxybutyrate) depolymerase (PhaZ7) from Paucimonas lemoignei. Acta Crystallogr. Sect. F Struct. Biol. Cryst. Commun. *61*, 479–481.

Latorre, R., Brauchi, S., Madrid, R., and Orio, P. (2011). A cool channel in cold transduction. Physiology (Bethesda) *26*, 273–285.

Liu, B., and Qin, F. (2005). Functional control of cold- and menthol-sensitive TRPM8 ion channels by phosphatidylinositol 4,5-bisphosphate. J. Neurosci. *25*, 1674–1681.

McKemy, D.D., Neuhausser, W.M., and Julius, D. (2002). Identification of a cold receptor reveals a general role for TRP channels in thermosensation. Nature *416*, 52–58.

Morenilla-Palao, C., Pertusa, M., Meseguer, V., Cabedo, H., and Viana, F. (2009). Lipid raft segregation modulates TRPM8 channel activity. J. Biol. Chem. *284*, 9215–9224.

Mukherjee, S., Hao, Y.-H., and Orth, K. (2007). A newly discovered post-translational modification—the acetylation of serine and threonine residues. Trends Biochem. Sci. *32*, 210–216.

Negoda, A., Negoda, E., and Reusch, R.N. (2010). Importance of oligo-R-3-hydroxybutyrates to S. lividans KcsA channel structure and function. Mol. Biosyst. *6*, 2249–2255.

Nilius, B., Mahieu, F., Karashima, Y., and Voets, T. (2007). Regulation of TRP channels: a voltage-lipid connection. Biochem. Soc. Trans. *35*, 105–108.

Norris, V., Bresson-Dumont, H., Gardea, E., Reusch, R.N., and Gruber, D. (2009). Hypothesis: poly-(R)-3-hydroxybutyrate is a major factor in intraocular pressure. Med. Hypotheses *73*, 398–401.

Pani, A., Dessì, S., Diaz, G., La Colla, P., Abete, C., Mulas, C., Angius, F., Cannas, M.D., Orru, C.D., Cocco, P.L., et al. (2009). Altered cholesterol ester cycle in skin fibroblasts from patients with Alzheimer's disease. J. Alzheimers Dis. *18*, 829–841.

Papageorgiou, A.C., Hermawan, S., Singh, C.B., and Jendrossek, D. (2008). Structural basis of poly(3-hydroxybutyrate) hydrolysis by PhaZ7 depolymerase from Paucimonas lemoignei. J. Mol. Biol. *382*, 1184–1194.

Pavlov, E., Zakharian, E., Bladen, C., Diao, C.T.M., Grimbly, C., Reusch, R.N., and French, R.J. (2005). A large, voltage-dependent channel, isolated from mitochondria by water-free chloroform extraction. Biophys. J. *88*, 2614–2625.

Peier, A.M., Moqrich, A., Hergarden, A.C., Reeve, A.J., Andersson, D.A., Story, G.M., Earley, T.J., Dragoni, I., McIntyre, P., Bevan, S., and Patapoutian, A. (2002). A TRP channel that senses cold stimuli and menthol. Cell *108*, 705–715.

Pertusa, M., Madrid, R., Morenilla-Palao, C., Belmonte, C., and Viana, F. (2012). N-glycosylation of TRPM8 ion channels modulates temperature sensitivity of cold thermoreceptor neurons. J. Biol. Chem. *287*, 18218–18229.

Phelps, C.B., and Gaudet, R. (2007). The role of the N terminus and transmembrane domain of TRPM8 in channel localization and tetramerization. J. Biol. Chem. *282*, 36474–36480.

Reinhardt, S., Handrick, R., and Jendrossek, D. (2002). The "PHB depolymerase inhibitor" of Paucimonas lemoignei is a PHB depolymerase. Biomacromolecules *3*, 823–827.

Reusch, R.N. (1989). Poly-beta-hydroxybutyrate/calcium polyphosphate complexes in eukaryotic membranes. Proc. Soc. Exp. Biol. Med. *191*, 377–381.

Reusch, R.N. (1999). Streptomyces lividans potassium channel contains poly-(R)-3-hydroxybutyrate and inorganic polyphosphate. Biochemistry *38*, 15666–15672.

Rohács, T., Lopes, C.M., Michailidis, I., and Logothetis, D.E. (2005). PI(4,5)P2 regulates the activation and desensitization of TRPM8 channels through the TRP domain. Nat. Neurosci. *8*, 626–634.

Seebach, D., and Fritz, M.G. (1999). Detection, synthesis, structure, and function of oligo(3-hydroxyalkanoates): contributions by synthetic organic chemists. Int. J. Biol. Macromol. *25*, 217–236.

Seebach, D., Brunner, A., Bürger, H.M., Schneider, J., and Reusch, R.N. (1994). Isolation and 1H-NMR spectroscopic identification of poly(3-hydroxybutanoate) from prokaryotic and eukaryotic organisms. Determination of the absolute configuration (R) of the monomeric unit 3-hydroxybutanoic acid from Escherichia coli and spinach. Eur. J. Biochem. *224*, 317–328.

Selvamurugan, N., Shimizu, E., Lee, M., Liu, T., Li, H., and Partridge, N.C. (2009). Identification and characterization of Runx2 phosphorylation sites involved in matrix metalloproteinase-13 promoter activation. FEBS Lett. *583*, 1141–1146.

Tyo, K.E., Zhou, H., and Stephanopoulos, G.N. (2006). High-throughput screen for poly-3-hydroxybutyrate in Escherichia coli and Synechocystis sp. strain PCC6803. Appl. Environ. Microbiol. *72*, 3412–3417.

Voets, T., Droogmans, G., Wissenbach, U., Janssens, A., Flockerzi, V., and Nilius, B. (2004). The principle of temperature-dependent gating in cold- and heat-sensitive TRP channels. Nature *430*, 748–754.

Xian, M., Fuerst, M.M., Shabalin, Y., and Reusch, R.N. (2007). Sorting signal of Escherichia coli OmpA is modified by oligo-(R)-3-hydroxybutyrate. Biochim. Biophys. Acta *1768*, 2660–2666.

Yudin, Y., and Rohacs, T. (2012). Regulation of TRPM8 channel activity. Mol. Cell. Endocrinol. *353*, 68–74.

Yudin, Y., Lukacs, V., Cao, C., and Rohacs, T. (2011). Decrease in phosphatidylinositol 4,5-bisphosphate levels mediates desensitization of the cold sensor TRPM8 channels. J. Physiol. *589*, 6007–6027.

Zakharian, E., and Reusch, R.N. (2004). Functional evidence for a supramolecular structure for the Streptomyces lividans potassium channel KcsA. Biochem. Biophys. Res. Commun. *322*, 1059–1065.

Zakharian, E., and Reusch, R.N. (2005). Kinetics of folding of Escherichia coli OmpA from narrow to large pore conformation in a planar bilayer. Biochemistry *44*, 6701–6707.

Zakharian, E., Thyagarajan, B., French, R.J., Pavlov, E., and Rohacs, T. (2009). Inorganic polyphosphate modulates TRPM8 channels. PLoS ONE *4*, e5404.

Zakharian, E., Cao, C., and Rohacs, T. (2010). Gating of transient receptor potential melastatin 8 (TRPM8) channels activated by cold and chemical agonists in planar lipid bilayers. J. Neurosci. *30*, 12526–12534.

Zhang, Z., Tan, M., Xie, Z., Dai, L., Chen, Y., and Zhao, Y. (2011). Identification of lysine succinylation as a new post-translational modification. Nat. Chem. Biol. *7*, 58–63.